COMBINING A MULTIRATE REPETITIVE LEARNING CONTROLLER WITH COMMAND SHAPING FOR IMPROVED FLEXIBLE MANIPULATOR CONTROL

Sungsoo Rhim
School of Mechanical Engineering
Georgia Institute of Technology
Atlanta, Georgia 30332
Email: gt5543a@prism.gatech.edu

Ai-Ping Hu
School of Mechanical Engineering
Georgia Institute of Technology
Atlanta, Georgia 30332
Email: gt0162c@prism.gatech.edu

Nader Sadegh
School of Mechanical Engineering
Georgia Institute of Technology
Atlanta, Georgia 30332
Email: nader.sadegh@me.gatech.edu

Wayne J. Book
School of Mechanical Engineering
Georgia Institute of Technology
Atlanta, Georgia 30332
Email: wayne.book@me.gatech.edu

ABSTRACT

Command shaping, a feedforward approach used to control flexible manipulators, performs most effectively when applied to a linear system. In practice, various nonlinearities are present in a given system that will deteriorate the performance of command shaping. In this work, a multirate repetitive learning controller (MRLC) is used in conjunction with a command shaping method known as the optimal arbitrary time-delay filter (OATF) for discrete-time joint control of a single flexible link manipulator containing nonlinearities. With very little a priori knowledge of the given system, a MRLC is able to cancel the nonlinearities at select frequencies and achieve near-perfect tracking of a periodic desired trajectory. By doing this, a MRLC controls the joint to follow a given shaped command more closely, thus allowing the OATF to more effectively attenuate residual tip vibrations. It is shown both analytically and experimentally that this controller is more effective than a conventional PID and OATF controller at attenuating residual tip vibrations.

INTRODUCTION

Having flexibility in a mechanical manipulator will degrade trajectory tracking control and manipulator tip positioning. In practice, however, constraints imposed by manufacturing and operating costs, as well as by various operating environments, will render the presence of such flexibility unavoidable.

Numerous researchers have proposed control schemes to attenuate tip vibration due to flexure during mechanical manipulator motion. These methods may be divided into two categories: feedback and feedforward. Feedback algorithms utilize measurement signals, whereas feedforward algorithms will only utilize desired reference signals. In this work, we will consider a particular feedforward method known as *command shaping*.

Command shaping seeks to reduce tip vibrations by reshaping the desired trajectory to be tracked in order to produce a new trajectory that will not excite the resonances of the flexible manipulator. Command shaping is advantageous because it is able to accomplish this task without regard to the particular form of the desired trajectory. Since its introduction (Singer and Seering, 1990), the command shaping method has been applied successfully in several different applications ((Magee and Book, 1994), (Rhim and Book, 1997)). In our work, we have used a particular command shaping method known as the *optimal arbitrary time-delay filter* (OATF) (Magee, 1996).

The effectiveness of command shaping relies on the linearity of the flexible manipulator system the (reshaped) desired trajectory is commanding. If this system is not linear, we will still observe excitation of the manipulator tip even when using a properly reshaped desired trajectory. The particular flexible mechanical manipulator we have used in our experiments is a gantry-type robot with a prismatic joint and a single flexible link. This is a configuration which is widely used in industry. It is often mod-

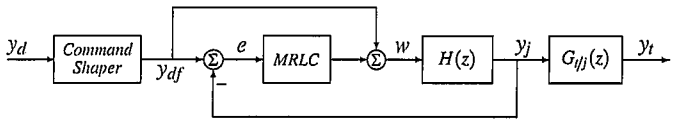

Figure 1. CONCEPTUAL BLOCK DIAGRAM WITH COMMAND SHAPING AND A MRLC.

eled as a linear system by neglecting nonlinear elements, such as friction in the joint. We have found, however, that there is a non-negligible amount of nonlinear friction and nonlinear actuation at the prismatic joint of our test bed robot. Application of command shaping to this system is thus made less effective.

The general approach we will be interested in taking to overcome this limitation of command shaping is to compensate for the nonlinear effects present in a given system. Khorrami et al. have used feedback linearization to linearize their joint control system for a two-link flexible manipulator, before applying command shaping (Khorrami et al., 1994). They then later incorporated adaptive nonlinear control algorithms to address scenarios in which parameters may be changing with time (Khorrami et al., 1995). The nonlinearity in their study is due to the configuration-dependent dynamics of a two-link system. These control schemes necessarily require detailed knowledge regarding one's system.

In this paper, we use a *multirate repetitive learning controller* (MRLC) to compensate for the nonlinearities in our flexible system before applying command shaping. A learning controller estimates, through practice, the control input required to theoretically achieve perfect tracking of a periodic desired trajectory. Unlike a typical adaptive control scheme, which often assumes a specific model of the plant and then seeks to estimate unknown constant parameters within that model, learning controllers require very little a priori knowledge regarding the plant to be controlled. Figure 1 shows the conceptual block diagram representing the discrete-time control system for our gantry-type robot with a prismatic joint and a single flexible link. y_d is the desired joint trajectory, y_{df} is the filtered desired joint trajectory, y_j is the joint displacement, y_t is the tip displacement, $e = y_{df} - y_j$, w is the control input to the asymptotically stabilized plant, $H(z)$, and $G_{t/j}(z)$ is the linear transfer function from joint displacement to tip displacement. The strategy is to use a MRLC to try to achieve perfect tracking of y_{df} by y_j (i.e., to get $y_j/y_{df} \approx 1$). Having accomplished this, our command shaper, the OATF, is then able to attenuate residual tip vibrations more effectively.

FLEXIBLE MANIPULATOR DYNAMICS

The system of interest to this work is the gantry-type robot with a prismatic joint and single flexible link shown schematically in Figure 2. $u(t)$ denotes the control force as a function of time, t. The length of the flexible link is L. The x-w frame is

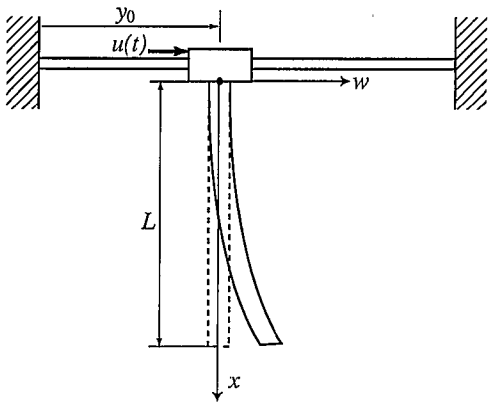

Figure 2. SCHEMATIC DIAGRAM OF THE GANTRY ROBOT WITH A FLEXIBLE LINK.

attached to the prismatic joint and moves with the flexible link. $y_0(t)$ represents the horizontal displacement of the joint. Then, the horizontal displacement of the flexible link at a given value of x can be expressed as

$$y(t,x) = y_0(t) + w(t,x). \tag{1}$$

The flexible link system consists of an infinite number of degrees of freedom. For practical purposes, however, we assume that we are able to characterize the system's behavior well enough with only N. Using the method of assumed modes, we thus have

$$y(t,x) = \sum_{i=1}^{N} q_i(t)\phi_i(x), \tag{2}$$

where $q_i(t)$ are generalized coordinates and $\phi_i(x)$ are basis functions. Then, e.g., by using Lagrange's equations, we find that the system's equations of motion are given by

$$M\ddot{q}(t) + D\dot{q}(t) + Kq(t) = Bu(t), \tag{3}$$

where,

$$M \equiv \begin{bmatrix} M_r & M_{re} \\ M_{re}^T & M_e \end{bmatrix}, \quad K \equiv \begin{bmatrix} 0 & 0 \\ 0 & K_e \end{bmatrix}, \quad D = \alpha M + \beta K, \quad B = \begin{bmatrix} 1 \\ 0 \end{bmatrix},$$

α and β are constants, and $q(t) = [q_r(t)\ q_e(t)]^T$, where $q_r(t)$ is the rigid generalized coordinate (representing the joint motion) and $q_e(t)$ are the flexible generalized coordinates (representing the flexible link motion). The subscripts r and e in the above equations denote rigid body motion and elastic motion, respectively; M_{re} represents coupling between the rigid mode and the

elastic modes. Only one rigid mode appears in the above equation corresponding to the horizontal translation. Generally, the mass matrix M and the stiffness matrix K may vary with the system configuration $q(t)$. However, for our gantry-type manipulator, these matrices are constant.

Note that the damping term ($D\dot{q}(t)$) is presently assumed to be linear. This is so that we may proceed in this section to obtain a nominal linear model of our system. The actual damping in our physical system is known to be nonlinear, due to nonlinear friction.

The manipulator joint displacement, $y_j(t)$, and the tip displacement, $y_t(t)$, are expressed in terms of the generalized coordinates by

$$y(t) \equiv \begin{bmatrix} y_j(t) \\ y_t(t) \end{bmatrix} = \begin{bmatrix} \Phi^T(0) \\ \Phi^T(L) \end{bmatrix} q(t), \tag{4}$$

where $\Phi(z)^T = [\phi_1(z)\ \phi_2(z)\ \cdots\ \phi_N(z)]$.

Next, we proceed to derive the transfer functions between the control force, $u(t)$, and the outputs $y(t)$. First, we observe that

$$\frac{Q_r(s)}{U(s)} = \frac{1 - \left(s^2 M_e + sD_{22} + K_{22}\right)^{-1} (sD_{12}K_{12}) B_2}{s^2 M_r + sD_{11}} \tag{5}$$

and

$$\frac{Q_e(s)}{U(s)} = \left(s^2 M_e + sD_{22} + K_{22}\right)^{-1} B_2, \tag{6}$$

where s is the Laplace variable and, e.g., $Q_r(s)$ is the Laplace transform of $q_r(t)$. Also,

$$D_{11} = \alpha M_r, \quad D_{12} = -\beta M_{re} {M_e}^{-1} K_e, \quad D_{22} = \alpha M_e + \beta K_e,$$
$$K_{12} = -M_{re} {M_e}^{-1} K_e, \quad K_{22} = K_e, \quad \text{and} \quad B_2 = -{M_{re}}^T / M_r.$$

Then, using equation (4), we obtain the transfer functions $G_j(s) \equiv Y_j(s)/U(s)$ and $G_t(s) \equiv Y_t(s)/U(s)$:

$$\begin{bmatrix} Y_j(s) \\ Y_t(s) \end{bmatrix} = \begin{bmatrix} \Phi^T(0) \\ \Phi^T(L) \end{bmatrix} \begin{bmatrix} Q_r(s) \\ Q_e(s) \end{bmatrix}, \tag{7}$$

$$\begin{bmatrix} G_j(s) \\ G_t(s) \end{bmatrix} \equiv \begin{bmatrix} Y_j(s)/U(s) \\ Y_t(s)/U(s) \end{bmatrix} = \begin{bmatrix} \Phi^T(0) \\ \Phi^T(L) \end{bmatrix} \begin{bmatrix} Q_r(s)/U(s) \\ Q_e(s)/U(s) \end{bmatrix}. \tag{8}$$

Thus, we see that the transfer function from joint displacement to tip displacement, $G_{t/j}(s)$, is given by

$$G_{t/j}(s) \equiv \frac{Y_t(s)/U(s)}{Y_j(s)/U(s)}. \tag{9}$$

COMMAND SHAPING

Description and Theory

A *command shaper* reshapes the desired input to a flexible system such that the resonances of the elastic system modes are not excited. It takes the form of a finite impulse response (FIR) filter, with filter parameters determined by the resonant frequencies and the damping ratios of the undesired elastic modes of the flexible system. For a linear time-invariant system, the command shaper first delays part of the input command, and then reshapes that delayed part in order to cancel the residual vibrations caused by previous command inputs.

In this research we have used a particular command shaping technique called the optimal arbitrary time-delay filter. For single elastic mode cancellation, the *three-term* OATF is given by the following equation (note that it requires that certain parameters of the elastic system be known in order to calculate the coefficients of the filter):

$$c(t) \equiv \frac{1}{M}(\delta(t) - 2\cos(\omega_d T_d) e^{-\zeta\omega_n T_d} \delta(t - T_d) + e^{-2\zeta\omega_n T_d} \delta(t - 2T_d)), \tag{10}$$

where T_d is the time delay (the time delay specifies the amount of time by which the input command is delayed), $\delta(t)$ is the unit impulse function centered at $t = 0$, ω_n is the first natural frequency of the flexible system, ζ is the corresponding damping ratio, ω_d is the corresponding damped natural frequency, and $M \equiv 1 - 2\cos(\omega_d T_d) e^{-\zeta\omega_n T_d} + e^{-2\zeta\omega_n T_d}$. What this particular FIR filter does is cancel the poles of the flexible system with filter zeros. In order to have the same total steady-state response both before and after the command shaping of the input, the command shaper is normalized to have unit DC gain. Magee (1996) shows that if the command shaper coefficients are properly chosen, the filter is capable of canceling the given resonance poles using any T_d; note that this is not true for earlier command shaping methods. The following equation gives the zeros of the OATF in the s-domain. Using any value of T_d, this filter has an infinite number of zeros, including the zeros at the locations of the resonance poles of the flexible system:

$$s = -\zeta\omega_n \pm j(\omega_d + \frac{2n\pi}{T_d}), \tag{11}$$

where $n = 0, \pm 1, \pm 2, \ldots$.

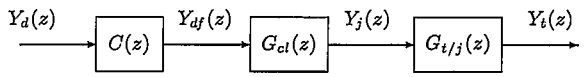

Figure 3. CONCEPT OF COMMAND SHAPING.

When we realize command shaping in the discrete-time domain, the time delay T_d is not permitted to be an arbitrary number. Instead, it must be chosen as an integer multiple of the plant sampling time, T. The freedom of the OATF in choosing the time delay makes it easy to implement in a digital control system. The z-domain representation of the OATF is given by

$$C(z) \equiv \frac{1}{M}(1 - 2\cos(\omega_d T_d)e^{-\zeta\omega_n T_d}z^{-\Delta} + e^{-2\zeta\omega_n T_d}z^{-2\Delta}), \quad (12)$$

where $\Delta = integer = T_d/T$.

Limitations When Applied to a Nonlinear System

Figure 3 illustrates the way in which we have implemented command shaping in our flexible manipulator system. We define the closed-loop system to be $G_{cl}(z) \equiv Y_j(z)/Y_{df}(z)$. Therefore,

$$Y_t(z) = Y_d(z)C(z)G_{cl}(z)G_t(z) = Y_{df}(z)G_{cl}(z)G_t(z), \quad (13)$$

and the vibration of the tip relative to the joint is

$$\begin{aligned} Y_{vib}(z) &\equiv Y_t(z) - Y_j(z) \\ &= Y_{df}(z)G_{cl}(z)(G_t(z) - 1). \end{aligned} \quad (14)$$

Note that if the closed-loop system is linear, as well as time- invariant, then the command shaper, $C(z)$, may be readily designed to cancel the resonance poles of $G_{t/j}(z)$. However, if instead the given closed-loop system is nonlinear, then the command shaper is rendered relatively ineffective at attenuating residual tip vibrations. We have verified this expected degradation in performance experimentally: since our physical system is characterized by a significant amount of (nonlinear) friction, we found that we were not able to achieve the best performance that command shaping is otherwise capable of. However, we were able to obtain relatively good results when we used a multirate repetitive learning controller. As we will see in the next section, the reason for this is because a MRLC is able to get rid of the disturbances at particular frequencies caused by nonlinear effects in the system.

MULTIRATE REPETITIVE LEARNING CONTROLLER

Repetitive learning controllers are effective in achieving precise tracking of periodic (i.e., strictly time-dependent) trajectories. In fact, a repetitive learning controller is theoretically able to achieve perfect tracking, even in the presence of system nonlinearities. We have implemented a *multirate* repetitive learning controller developed by James et al. ((James, 1997), (James and Sadegh, 1999), (James et al., 1999)) in the discrete-time domain for the task of accurately positioning the joint of our flexible manipulator system. Our objective in employing the MRLC is that it has the ability to cancel the nonlinearities in a given system at select frequencies. This will be shown in the analysis to follow.

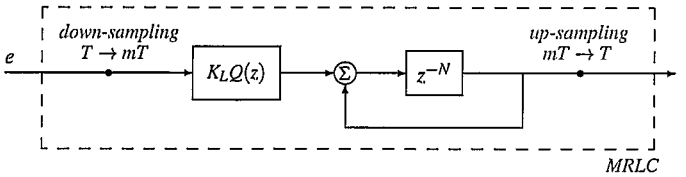

Figure 4. MULTIRATE REPETITIVE LEARNING CONTROLLER.

In a multirate scheme, the learning controller samples at a slower rate than the plant, whereas in a single-rate scheme the controller and plant have the same sample rate. The order of a discrete-time repetitive learning controller is directly proportional to its sample rate and to the period of the desired trajectory to be tracked. A discrete repetitive learning controller which has too high a sample rate may exhibit undesirable high frequency characteristics, be unstable, and incur excessive memory storage costs. By sampling at a relatively slower rate, a MRLC seeks to avoid such potential problems, without the need to have the plant's sample rate slowed down. Sadegh (1991, 1995) has formulated stability criteria for single-rate repetitive learning controllers and James et al. (1999) have extended the single-rate results to the multirate case.

Figure 4 shows the block diagram representing the general form of the MRLC. T is the plant sample period and m is an integer greater than 1. *Down-sampling* refers to switching from a faster sampling rate to a slower sampling rate and *up-sampling* refers to switching from a slower sampling rate to a faster sampling rate. We have implemented down-sampling using a linear weighted average and up-sampling using linear interpolation.

The MRLC is of the form $K_L Q(z)R(z)$, where $K_L > 0$ is the *learning gain*, $Q(z)$ is a lead compensator, and $R(z) \equiv 1/(z^N - 1)$, which is a NmT time-delay positive feedback loop, where NmT is the period of the desired trajectory to be tracked. We require that K_L and $Q(z)$ be chosen such that the following multirate repetitive learning control stability criterion is satisfied (James et al., 1999).

Theorem 1. *Let $H(z)$ be the transfer function of an asymptotically stable plant sampling at the rate $1/T$ and subject to up-sampling and down-sampling at its boundaries. Denoting the slower-rate (i.e., $\frac{1}{mT}$) equivalent of $H(z)$ by $H^*(z)$, then the closed-loop repetitive learning control system, with the repetitive learning controller sampling at $\frac{1}{mT}$, is asymptotically stable*

if the following two conditions are met.

1. $Re(Q(a_i)H^*(a_i)) > 0$, *for* $i = 0,1,2,\ldots,N-1$ *and* $a_i \equiv \exp(\frac{2\pi j}{N} i)$.
2. $K_L \leq 2$ *is chosen such that there is no encirclement of* -1 *in the complex plane by the Nyquist diagram of* $z^{-N}(K_L Q(z)H^*(z) - 1)$.

Essentially, in a system containing multiple sample rates, an equivalent plant which samples at the same (slower) rate as the repetitive learning controller is first formulated. This then permits single-rate repetitive learning control stability results to be applied.

$R(z)$ may be expressed as the sum of N first-order transfer functions:

$$R(z) = \sum_{i=0}^{N-1} \frac{c_i}{z - a_i}, \tag{15}$$

where c_i is the ith undetermined coefficient and $a_i = \exp(\frac{2\pi j}{N} i)$ are the pole locations. a_0 is called the *fundamental frequency* and the $N-1$ integer multiples of the fundamental frequency are the *harmonic frequencies*. It is assumed that the frequency components of the periodic desired trajectory are contained within these N frequencies. If this is the case, then, theoretically, (for the single-rate case) repetitive learning control provides tracking error reduction to zero by putting infinite gains in the feedforward loop at the particular frequencies of the desired trajectory. Thus, ideally, a repetitive learning controller will have the effect of making the closed-loop transfer function $Y_j(z)/Y_{df}(z)$ (or $Y_j(z)/Y_d(z)$, if the desired trajectory is not being filtered) unity at the fundamental frequency and the $N-1$ harmonic frequencies. In the multirate case, however, we find that there will be some form of resolution loss at the boundaries where the sample rates change. As we now show, this has the effect of causing the closed-loop transfer function to only approximate unity at the fundamental frequency and the $N-1$ harmonic frequencies.

Consider the block diagram in Figure 5, which is a representation of the control system we have implemented. Note that this is an equivalent system to the one shown in Figure 1. $A(z)$ is a linear weighted averaging filter, * denotes down-sampling, K_L is the learning gain, $R^*(z) = 1/(z^N - 1)$, and $I(z)$ is the linear interpolation (up-sampling) filter. Then,

$$\begin{aligned} V(z) &= A(z)D(z)(Y_{df}(z) - Y_j(z)) \\ &= A(z)D(z)(1 - G_c(z)D(z))Y_{df}(z) \\ &\quad -K_L A(z)D(z)G_c(z)I(z)R^*(z)V^*(z), \end{aligned} \tag{16}$$

where, $G_c(z) \equiv G_p(z)/(1 + G_p(z)D(z))$. Down-sampling both

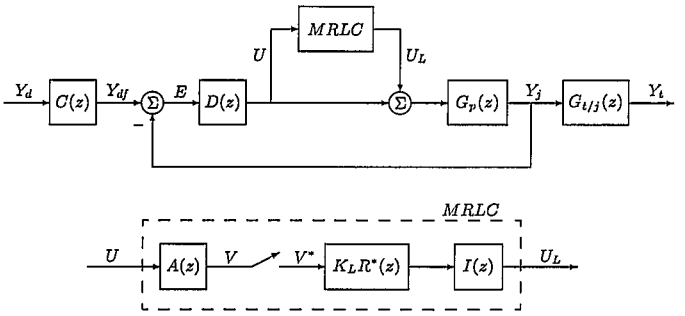

Figure 5. BLOCK DIAGRAM OF ACTUAL CONTROL SYSTEM IMPLEMENTED.

sides of equation (16) yields

$$\begin{aligned} V^*(z) &= H_d^*(z)Y_{df}^*(z) - K_L H^*(z)R^*(z)V^*(z) \\ &= \frac{H_d^*(z)}{1 + K_L H^*(z)R^*(z)V^*(z)} Y_{df}^*(z) \\ &= \frac{(z^N - 1)\,H_d^*(z)}{z^N - 1 + K_L H^*(z)V^*(z)} Y_{df}^*(z), \end{aligned} \tag{17}$$

where $H_d(z) \equiv A(z)D(z)I(z)/(1 + G_p(z)D(z))$ and $H(z) \equiv A(z)D(z)G_c(z)I(z)$. $H(z)$ represents the asymptotically-stabilized plant that was referred to in Figure 1 and in **Theorem 1**. Here, $Y_{df}(z)$ is assumed to be the output of an up-sampler, that is: $Y_{df}(z) = I(z)Y_{df}^*(z)$. Therefore,

$$\begin{aligned} Y_j(z) &= G_c(z)D(z)Y_{df}(z) \\ &\quad + K_L^2 G_c(z)I(z)R^*(z)\frac{R^*(z)H_d^*(z)}{1 + K_L R^*(z)H^*(z)} Y_{df}^*(z). \end{aligned} \tag{18}$$

The closed-loop transfer function is then

$$\frac{Y_j(z)}{Y_{df}(z)} = G_c(z)\left(D(z) + \frac{R^*(z)H_d^*(z)}{1 + R^*(z)H^*(z)}\right). \tag{19}$$

At the fundamental frequency a_0 and at the harmonic frequencies a_i, for $i = 1,2,\ldots,N-1$, we find that

$$(V^*(z))_{z=a_i} = ((A(z)D(z)E(z))^*)_{z=a_i} = 0. \tag{20}$$

If $D(z)$ is chosen sufficiently large, $E(z) = Y_{df}(z) - Y_j(z)$ is guaranteed to be very close to zero, which means that

$$\left(Y_j(z)/Y_{df}(z)\right)_{z=a_i} \approx 1. \tag{21}$$

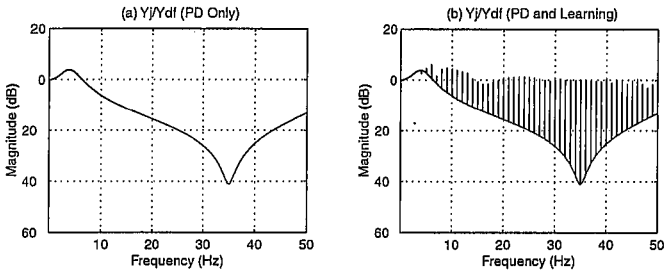

Figure 6. BODE PLOTS OF $Y_j(z)/Y_{df}(z)$ FOR 'PID ONLY' CASE AND 'PD AND LEARNING' CASE.

Our flexible manipulator system has two outputs of interest: joint displacement and tip displacement. Controlling tip displacement is especially important since practically all of the manipulator's detailed work is performed at that end. Thus, the precision of the performed task is generally dictated by the precision of the tip motion.

In this work, we assume that only joint displacement is measured and available for feedback. There is no way to directly control tip motion. Instead, we seek to indirectly control tip motion by using joint control. As we have shown, a MRLC possesses characteristics that cause the closed-loop transfer function between the measured joint displacement and the desired joint trajectory to be approximately unity at a certain fundamental frequency and at given harmonic frequencies. This is demonstrated in Figure 6. Plot (a) shows the magnitude of the closed loop transfer function of a flexible manipulator with a single rigid mode and a single elastic mode when a proportional-derivative (PD) feedback controller is used. Plot (b) shows the result of applying to this system a MRLC which has a fundamental frequency of 1 Hz and a down-sampling ratio of 5. A comparison of the two plots shows the advantage of using a MRLC compared to using PD only. The magnitudes at the fundamental frequency and at the harmonic frequencies are approximately unity.

However, we see that the "peaks" in magnitude evident in plot (b) will be added onto the magnitude of the transfer function between tip displacement and joint displacement ($G_{t/j}(z)$), and will thus amplify the gains between these two signals. Therefore, application of a MRLC alone has the effect of greatly improving joint position tracking at the cost of increasing unwanted tip vibrations.

EXPERIMENTS

System Description

The flexible mechanical manipulator we have used in our experiments is the gantry-type pick-and-place robot shown in Figure 7. The system contains two prismatic joints. The first one is to constrain the motion of the *main head* to be along the horizontal track of the *linear motor*. The displacement of the main head

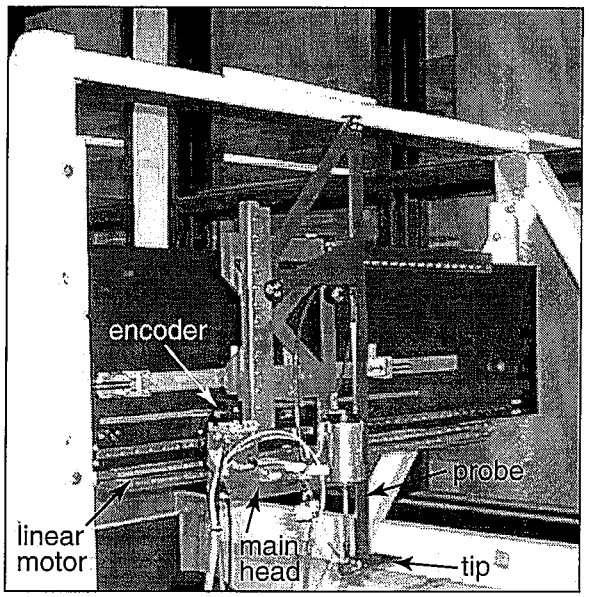

Figure 7. PICTURE OF THE TEST BED: GANTRY ROBOT WITH A SINGLE FLEXIBLE LINK.

corresponds to $y_j(t)$ and is measured with an *encoder*. The resolution of this encoder is 1 μm. The second prismatic joint moves the *probe* (i.e., the flexible link) vertically. Since our work is concerned only with horizontal motions, this second joint is held fixed throughout our experiments. The horizontal displacement of the *tip* of the probe corresponds to $y_t(t)$. We use a piezoelectric accelerometer attached to the tip in order to measure horizontal tip vibration. With a 2 kg payload affixed to its tip, the probe has a single dominant elastic mode with a natural frequency of approximately 35 Hz. The OATF command shaper we designed is based on this and other parameters obtained from system identification experiments.

We have implemented our controllers digitally, using a 1 kHz sample rate. For the MRLC, we have used a down-sampling ratio of 5. Only main head displacement measurements, as measured by the encoder, are used in our control algorithms; the accelerometer measurements are used only as an indicator of control system performance.

Joint Displacement

The periodic desired trajectory, $y_d(t)$, we have used in our experiments is shown in Figure 8. It is an offset sinusoid alternating with zero-velocity segments. The amplitude of displacement is 5×10^4 μm and the period is 1 second. Also shown are the first two derivatives of $y_d(t)$.

We have implemented the following four different joint controllers experimentally.

1. PID: proportional-integral-derivative feedback controller

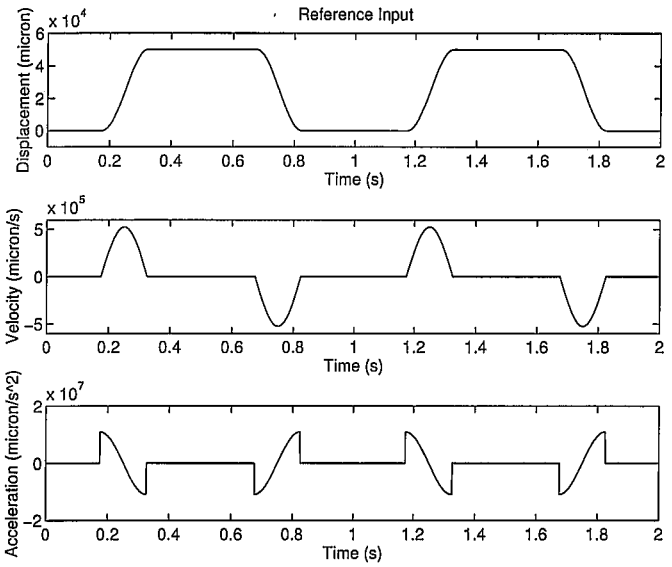

Figure 8. DESIRED POSITION, VELOCITY, AND ACCELERATION.

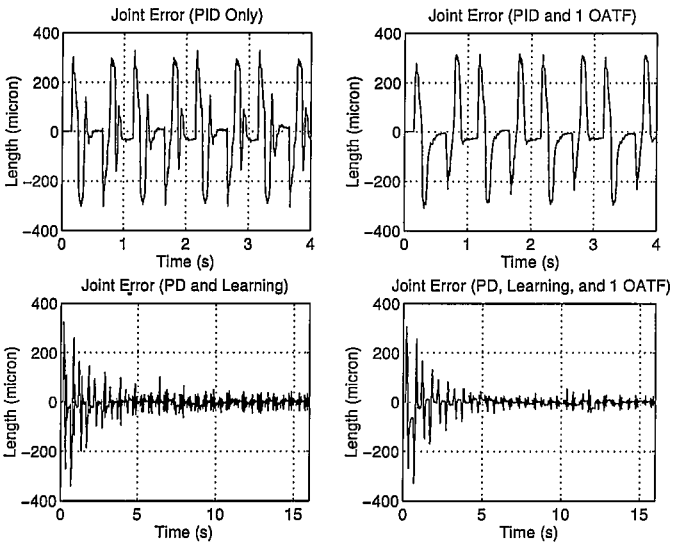

Figure 9. COMPARISON OF JOINT ERROR USING FOUR DIFFERENT CONTROL ALGORITHMS.

based on joint error.

2. PID and OATF: PID with the OATF command shaper implemented.
3. PD and Learning: MRLC combined with a PD controller.
4. PD, Learning, and OATF: MRLC combined with a PD controller, and with the OATF command shaper implemented.

The joint tracking error obtained for each of the four cases is shown in Figure 9. Both the 'PID' case and the 'PID and OATF' case have errors of maximum ± 300 μm. These errors exhibit very strong periodicity. Thus, when learning control is applied, we see that we are able to reduce the joint tracking error down to about ± 30 μm after several cycles of learning.

The addition of a command shaper has the effect of reshaping the desired trajectory, thus making it smoother. This results in smaller required joint accelerations, which explains the small differences in the error plots between the cases with the OATF and the cases without the OATF.

Tip Vibration

We have also measured tip acceleration for each of our four control cases. The results are shown in Figure 10.

It is evident that the addition of the OATF to PID is effective at attenuating residual tip vibration. It is also evident that in the 'PD and Learning' case, the residual tip vibration is relatively increased compared to the 'PID' case. The reason for this is because, as we saw in Section 4, when a learning controller is applied (without there being an OATF), the result is that the magnitude of the closed-loop system increases (i.e., we found that $|(G_{cl})_{MRLC}| > |(G_{cl})_{PD}|$). The best results are obtained with 'PD, Learning, and OATF'. However, using the same reasoning as just

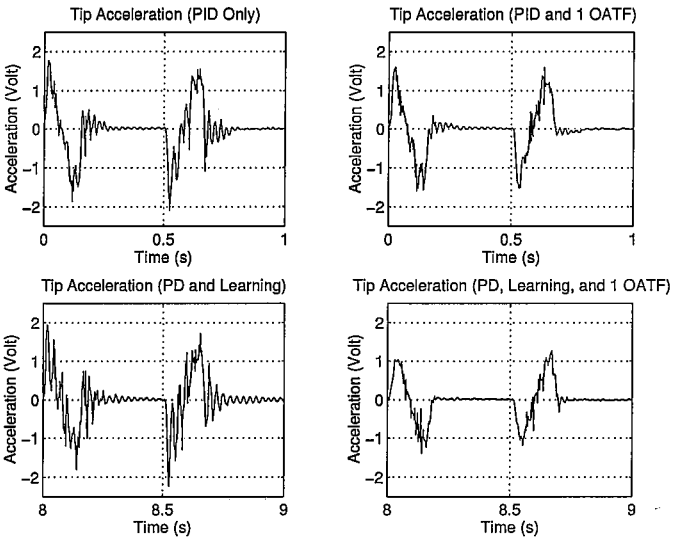

Figure 10. COMPARISON OF TIP ACCELERATION USING FOUR DIFFERENT CONTROL ALGORITHMS.

above, we should expect that the best results would come from the 'PID and OATF' case, instead. This apparent discrepancy is explained by the fact that our analysis did not account for nonlinearities present in our system; principally, nonlinear friction. As we've seen, unlike the PID controller, the MRLC partially cancels nonlinearities. Thus, the joint position $y_j(t)$ will closely follow $y_{df}(t)$, which permits the OATF to perform its task more effectively.

CONCLUSIONS

We have combined the OATF command shaping method with a multirate repetitive learning controller for application to the control of a flexible mechanical manipulator. Our controllers were implemented on a gantry-type flexible robot containing nonlinear friction; the outputs of interest are joint displacement and flexible link tip displacement. We have shown, both theoretically and experimentally, that the MRLC is able to partially linearize the closed-loop dynamics of our system by dramatically decreasing joint tracking error. Since the OATF is effective only for the case of a linear closed-loop system, we have found that for our flexible manipulator the performance of the OATF is greatly improved when used in conjunction with the MRLC.

ACKNOWLEDGEMENTS

The authors thank Professor Stephen Dickerson at the Georgia Institute of Technology for his helpful advice and insight pertaining to this work. The control approach described in this paper has been patented by the Georgia Institute of Technology. This research has been partially supported by CAMotion, Inc..

REFERENCES

James, C. D., *The Design of Robust Multi-rate Repetitive Learning Controllers with Applications to Practical Systems*, Ph.D. thesis, Georgia Institute of Technology, Atlanta, GA, November 1997.

James, C. and N. Sadegh, "Synthesis and Stability of a Multirate Repetitive Learning Controller," *Proceedings of the American Control Conference*, San Diego, CA, June 2–4, 1999, pp. 358–362.

James, C., N. Sadegh and A.-P. Hu, "Synthesis, Stability Analysis, and Experimental Implementation of a Multirate Repetitive Learning Controller," to appear in *Proceedings of the IEEE/ASME International Conference on Advanced Intelligent Mechatronics*, Atlanta, GA, September 19–23, 1999.

Khorrami, F., S. Jain and A. Tzes, "Experiments on Rigid-body Based Controllers with Input Preshaping for a Two-link Flexible Manipulator," *IEEE Transactions on Robotics and Automation*, Vol. 10, no. 1, 1994, pp. 55–65.

Khorrami, F., S. Jain and A. Tzes, "Experimental Results on Adaptive Nonlinear Control and Input Preshaping for Multi-link Flexible Manipulators," *Automatica*, Vol. 31, no. 1, 1995, pp. 83–97.

Magee, D. P. and W. J. Book, "Filtering Schilling Manipulator Commands to Prevent Flexible Structure Vibration," *Proceedings of the American Control Conference*, Baltimore, MA, June 29 – July 1, 1994, pp. 2538–2542.

Magee, D. P., *Optimal Arbitrary Time-delay Filtering to Minimize Vibration in Elastic Manipulator Systems*, Ph.D. thesis, Georgia Institute of Technology, Atlanta, Georgia, August 1996.

Rhim, S. and W. J. Book, "Vibration Cancellation in Complex Support Structures for Precision Robots," *Proceedings of the ASME International Mechanical Engineering Congress and Exposition*, Dallas, TX, November 16–21, 1997, DSC-Vol. 61, pp. 503–509.

Sadegh, N., "Synthesis and Stability Analysis of Repetitive Controllers," *Proceedings of the American Control Conference*, Boston, MA, June 26–28, 1991, pp. 2634–2639.

Sadegh, N., "Synthesis of a Stable Discrete-time Repetitive Controller for MIMO Systems," *Journal of Dynamic Systems, Measurement, and Control*, Vol. 117, no. 1, 1995, pp. 92–98.

Singer, N. C. and W. P. Seering, "Preshaping Command Inputs to Reduce System Vibration," *Journal of Dynamic Systems, Measurement, and Control*, Vol. 112, no. 1, 1990, pp. 76–82.